

# New effective nuclear forces with a finite-range three-body term and their application to AMD+GCM calculations

Y. Kanada-En'yo

*Institute of Particle and Nuclear Studies,  
High Energy Accelerator Research Organization,  
1-1 Oho, Tsukuba, Ibaraki 305-0801, Japan*

Y. Akaishi

*Institute of Particle and Nuclear Studies,  
High Energy Accelerator Research Organization,  
1-1 Oho, Tsukuba, Ibaraki 305-0801, Japan*

We propose new effective inter-nucleon forces with a finite-range three-body operator. The proposed forces are suitable for describing the nuclear structure properties over a wide mass number region, including the saturation point of nuclear matter. The forces are applied to microscopic calculations of  $Z = N$  ( $A \leq 40$ ) nuclei and O isotopes with a method of antisymmetrized molecular dynamics. We present the characteristics of the forces and discuss the importance of the finite-range three-body term.

## I. INTRODUCTION

Experimental information concerning nuclear structure has been rapidly increasing in the region of unstable nuclei as well as stable nuclei. Together with the increase of experimental data, microscopic calculations of nuclear structure have developed to describe those structure properties. For a systematic study of various types of structures covering a wide region of the nuclear chart, the key issue in microscopic approaches is an extension of the model space. Corresponding to the advancement of microscopic calculations, one must improve the effective forces so as to be suitable for extended model space.

One of the basic properties of nuclei is saturation of the binding energy and density. The saturation property implies that a nucleus can be divided into fractional nuclei, and that such nuclei can fuse into a unified nucleus with only a small amount of energy. This “easiness of assembling and disassembling nucleons” [1] is one of the fundamental features of the nuclear many-body system. In nuclear-structure problems, this dynamics appears as a variety of structures such as clustering of nucleons and mean-field formation. Indeed, it is known that there exist many cluster states not only in stable nuclei, but also in unstable nuclei. This means that the basic dynamics of the nuclear structure contains two very different fundamentals. One is the formation of clusters, and the other is the formation of a mean field. With the traditional microscopic approaches, it was difficult to describe both of the features in one framework because of the limitation of the model space. Typical mean-field approaches, such as Hartree-Fock(HF) methods, are applicable to studying the mean-field aspect in the heavy nuclear region, while they are not suitable for studying cluster structure in light nuclei. On the other hand, cluster features in light stable nuclei were studied by cluster models. Recently, hybrid models, which can describe both the cluster aspect and the mean-field aspect, were developed and applied to structure studies of unstable nuclei as well as stable nuclei. One of the powerful approaches is a method of antisymmetrized molecular dynamics(AMD) [2,3], which is able to describe two different dynamics, i.e. the clustering and the mean-field formation due to its ab initio nature. In the study of unstable nuclei in the  $p$ -shell and  $sd$ -shell regions, performed with the AMD [1–3] method, it was found that both the cluster features and mean-field are essential in a systematic study of the ground and excited states of unstable nuclei as well as stable nuclei. As for an extended model based on three-dimensional HF calculations [4,5], a variation after the parity-projection method [6] might describe a variety of structures in light nuclei. In a systematic study with such extended models, the quality of the adopted effective interactions becomes an increasingly serious problem, because the structure is based on balance and competition between two different dynamics, like cluster formation and mean-field formation. This means that some theoretical results are sensitive to the adopted effective force, namely the Hamiltonian, which governs the system. In other words, the effective force must be appropriate to describe the characteristics of various states which may appear in the extended model space.

In microscopic calculations of nuclear structure, one often uses the effective forces to solve nuclear many-body problems. In most of the phenomenological effective inter-nucleon forces, the dominant part is expressed by central forces. With the Minnesota force [7] and the Volkov force [8], which consist of two-body central forces, the properties of very light nuclei are well reproduced. However, it is impossible to describe the saturation property of nuclear matter and heavy nuclei (mass number  $A \geq 10$ ) with such two-body central forces. For satisfying the saturation

properties, phenomenological density-dependent repulsive terms are usually imported in addition to the central two-body terms. Such forces with a density dependence are Gogny forces [9], Skyrme-type forces [11,10] and Modified Volkov forces [12], for example. These forces contain zero-range density-dependent operators or zero-range three-body operators. HF calculations with Gogny forces and Skyrme forces have succeeded in describing the bulk properties of the low-lying states of heavy nuclei. These forces, however, fail to reproduce the properties of very light nuclei. Tohsaki introduced repulsive terms with finite-range three-body operators, and proposed new effective forces responsible for the microscopic  $\alpha$ -cluster model, which succeeded to describe the overall properties over a wide range of masses from  $\alpha$  to nuclear matter [13]. Namely, the  $\alpha$ - $\alpha$  scattering behavior, the size and energy of double closed shell nuclei ( $\alpha$ ,  $^{16}\text{O}$  and  $^{40}\text{Ca}$ ) and the matter saturation property were successfully reproduced with Tohsaki's forces. However, unfortunately, the forces contain too complicated three-body operators to be employed in practical microscopic calculations of general nuclei.

Our aim in this paper is to propose new effective inter-nucleon forces which are applicable to practical calculations of general nuclei with the AMD method. In order to save computational costs, we introduce a simple three-body operator expressed by a one-range Gaussian. The new forces are applied to microscopic calculations of  $Z = N$  nuclei up to  $^{40}\text{Ca}$  and neutron-rich O isotopes with the AMD method. We explain the characteristics of the proposed forces and prove the success in describing the overall properties from the  $\alpha$  particle to nuclear matter, by demonstrating the results of the radii and energy of finite nuclei, the elastic  $\alpha$ - $\alpha$  scattering phase shift, and the saturation property of nuclear matter. We point out the significance of finite-range three-body terms in the effective forces from a phenomenological point of view, and discuss the role of the repulsive three-body terms in the connection with the tensor force, which is the origin of matter saturation.

This paper is organized as follows. The new effective forces with a finite-range three-body term are proposed in II. We describe the characteristics of the effective forces by demonstrating the calculated results with the new forces in III. In IV, the significant role of the finite-range three-body term is discussed. Finally, in V we summarize the present work.

## II. EFFECTIVE CENTRAL FORCES

As mentioned above, for most of the phenomenological effective forces in microscopic models, the dominant part is the central force. Concerning the effective central forces, it is regarded as a tensor force, a hard core and other terms in the bare interactions are renormalized because it is not easy to explicitly treat such terms in microscopic models for a nuclear many-body system. By categorizing the effective central forces into three types, we briefly review the general tendency of the typical effective forces to reproduce the structure properties, such as the saturation behaviour of nuclei and nuclear matter and the  $\alpha$ - $\alpha$  inter-cluster potential.

(1) Regarding finite-range two-body forces with no density-dependent terms, there exist such effective forces as Minnesota [7] and Volkov [8] forces which can reproduce the  $\alpha$ - $\alpha$  phase shift and the size and binding energy of an  $\alpha$  particle and light  $p$ -shell nuclei. However it is impossible to represent the saturation of matter and heavy nuclei with such the two-body central forces.

(2) Gogny [9] forces, Skyrme-type [10,11] forces and Modified Volkov [12] forces, which can guarantee nuclear matter saturation, contain zero-range density-dependent terms or zero-range three-body terms. Gogny forces and Skyrme-type forces successfully explain the size and the binding energy of the overall heavy nuclei, and also matter saturation. In spite of the success of nuclear matter saturation, all of these effective forces fail to reproduce the size of the  $\alpha$  particle and the  $\alpha$ - $\alpha$  scattering behaviour. Namely, all of these forces give larger  $\alpha$ -particle sizes and a less  $\alpha$ - $\alpha$  inter-cluster potential than the experimental ones. Therefore, the applicability of such forces to very light nuclei is not assured.

(3) We know only one kind of the effective force which can simultaneously guarantee the size of  $\alpha$  particle, the  $\alpha$ - $\alpha$  phase shift, and the saturation properties of nuclei and nuclear matter. That is the third type of effective force containing finite-range three-body operators, proposed by Tohsaki [13], namely, Tohsaki's F1 and F2 forces. It was found that these effective forces can successfully reproduce the  $\alpha$ - $\alpha$  phase shift, the sizes and binding energy of double-closed nuclei up to  $^{40}\text{Ca}$  and also matter saturation point.

In the present paper, we propose new effective forces which can be classified into the last category (3), forces with finite-range three-body operators. To reproduce the nuclear matter saturation properties, the effective central forces must contain density-dependent terms. It is considered that the origin of the density-dependent terms is suppression of the tensor force of bare nucleon-nucleon interactions in the nuclear matter. In other words, the density-dependent terms are considered to phenomenologically simulate the medium effect that tensor force is suppressed in the nuclear matter because of the Pauli principal. From this point of view, it seems to be reasonable that the effective central forces contain finite-range three-body terms because the original tensor force is the middle-range one. Moreover, the

TABLE I. Parameter sets of the effective central force(F3B force) in Eq. 1.

$v_1^{(2)}$ (MeV)	$v_2^{(2)}$ (MeV)	$a_1^{(2)}$ (fm)	$a_2^{(2)}$ (fm)	$v_3^{(2)}$ (MeV)	$a_3^{(2)}$ (fm)	$v^{(3)}$ (MeV)	$a^{(3)}$ (fm <sup>2</sup> )	$m$	$b$	$h$	
-198.34	300.86	1.2	0.7	22.5	0.9	600	1.25	case(1)	0.421	0.1	0.085
								case(2)	0.193	-0.185	0.37

type (2) forces with zero-range density-dependent terms have a fatal difficulty in simultaneously describing the density and the energy of an  $\alpha$  particle and nuclear matter. This failure in the quantitative reproduction of the saturation properties with type (2) forces is proved later in IV.

We propose effective central forces,  $V_{central}$ , expressed by two-body and three-body operators as follows:

$$V_{central} = \sum_{i<j} V_{ij}^{(2)} + \sum_{i<j<k} V_{ijk}^{(3)}, \quad (1)$$

where

$$V_{ij}^{(2)} = (1 - m + bP_\sigma - hP_\tau - mP_\sigma P_\tau) \sum_{n=1}^2 \left\{ v_n^{(2)} \exp \left[ -\left( \frac{\mathbf{r}_i - \mathbf{r}_j}{a_n^{(2)}} \right)^2 \right] \right\} + v_3^{(2)} \exp \left[ -\left( \frac{\mathbf{r}_i - \mathbf{r}_j}{a_3^{(2)}} \right)^2 \right] \quad (2)$$

$$V_{ijk}^{(3)} = v^{(3)} \exp \left[ -\frac{1}{a^{(3)}} \{ (\mathbf{r}_i - \mathbf{r}_j)^2 + (\mathbf{r}_j - \mathbf{r}_k)^2 + (\mathbf{r}_k - \mathbf{r}_i)^2 \} \right]. \quad (3)$$

$$(4)$$

Here we adopt a simple operator for the finite-range three-body terms. Compared with Tohsaki's forces expressed by three-range three-body operators, this one-range three-body operator with a symmetric form in the present forces is suitable for practical microscopic calculations of general nuclei with the AMD method.

We propose a set of parameters for the ranges and strengths of the two-body and three-body terms. The dominant components of the two-body terms are the first term in Eq.2. We adopt the same form as the Volkov force for this term, which consists of a medium-range attractive Gaussian and a short-range repulsive Gaussian. Wigner, Bertlett, Heisenberg and Majorana terms are chosen to be same parameters as the common multiplier of these two range Gaussians. The basic idea of the derivation of the parameters is that the nuclear structure properties over a wide mass number region should be described with a two-range two-body force and an one-range three-body force without mass-number depending parameters. We adopt the same range parameters for the two-range Gaussian of the two-body force as the Gogny force ( $a_1^{(2)} = 1.2(\text{fm})$  and  $a_2^{(2)} = 0.7(\text{fm})$ ). With longer range parameters, we failed to obtain sufficient reproduction of the nuclear structure. Although these range parameters for the two-body terms are shorter than the Volkov and MV1 forces, the range of the inter-cluster potential is not so different from those given by the MV1 forces, as shown in later, due to the effect of the repulsive finite-range three-body term in the present force. In order to explain the nucleon-nucleon scattering phase shift, the form with a two-range two-body and an one-range three-body is too simple because of the restriction of the simplified three-body operator. We add a small amount of a repulsive two-body term given by the second term of the two-body force in eq.2,  $v_3^{(2)} \exp \left[ -(\mathbf{r}_i - \mathbf{r}_j)^2 / a_3^{(2)^2} \right]$ , and tune again the strength of this term and the three-body term. In table I, the proposed parameter sets of the present forces are presented. We call the present parametrization as the F3B forces. Two sets case(1) and case(2) of parameters of  $m$ ,  $b$  and  $h$  for Wigner, Bertlett, Heisenberg and Majorana terms are listed in table I. Comparing the case(1) and case(2) parameters, the triplet and singlet even components are same but the odd components different between two sets (1) and (2). As a result, the case(1) and case(2) interactions give the same results for double closed  $Z = N$  nuclei written by HO wave functions, the  $\alpha$ - $\alpha$  interaction, and total energy of symmetric nuclear matter, however, they give different results for  $Z \neq N$  nuclei.

The present parameters  $m$  for the Majorana term shown in table I are determined so as to reproduce the binding energy of  $Z = N$  nuclei in mass region  $A = 4 \sim 40$  with the present AMD+GCM calculations. The Majorana parameter  $m$  is considered to be an adjusting parameter in fine tuning to fit the experimental data. It means that one can modify the value  $m$ , which is suitable to his model wave function.

In practical AMD calculations of  $Z = N$  nuclei and O isotopes, we also employ the two-body spin-orbit force in addition to these central F3B forces.

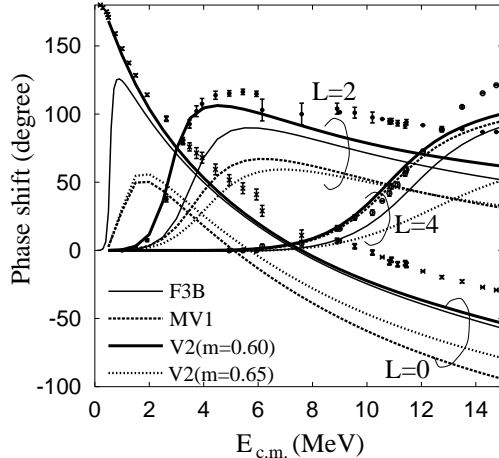


FIG. 1. Calculated phase shift of elastic  $\alpha$ - $\alpha$  scattering with the F3B force, the MV1 case 1( $m = 0.60$ ), and the Volkov No.2 ( $m = 0.60$  and  $m = 0.65$ ). The width parameter( $\nu$ ) for an  $\alpha$  particle in an RGM calculation was chosen to be 0.257, 0.209, 0.267 ( $\text{fm}^{-2}$ ) for the F3B, MV1, Volkov No.2 forces, respectively. The points indicate the experimental data taken from [16].

### III. CHARACTERISTICS OF THE EFFECTIVE FORCES

In this section, we exhibit the characteristics of the proposed effective forces concerning the saturation properties and  $\alpha$ - $\alpha$  scattering behavior compared with other types of typical phenomenological effective forces.

#### A. $\alpha$ - $\alpha$ interaction

The  $\alpha$ - $\alpha$  inter-cluster interaction is important for studying the cluster structure of light nuclei. The scattering phase shift is a useful physical quantity to inspect the features of the inter-cluster interaction. The phase shift of the elastic  $\alpha$ - $\alpha$  scattering is calculated by the resonating group method(RGM), where an  $\alpha$  particle is simply written using a  $(0s)^4$  harmonic oscillator wave function [14]. The width parameter of  $\alpha$  clusters is chosen to be the optimum value for an isolate  $\alpha$ -particle for each effective force.

In Fig. 1, the calculated  $\alpha$ - $\alpha$  phase-shift values are compared with the experimental data. It has been known that the experimental phase-shift data are well reproduced by the Minnesota force [7] and the Volkov No.2 force( $m = 0.60$ ) [15]. The theoretical values calculated with the new force(F3B) agree reasonably well with the experimental data. On the other hand, the MV1 case(1) force( $m = 0.60$ ) underestimates the experimental data, which means that the force provides a less-attractive  $\alpha$ - $\alpha$  interaction. It was also found that the SII force(a Skyrme-type force) gives a less-attractive inter- $\alpha$  interaction, and therefore, fails to reproduce the  $\alpha$ - $\alpha$  phase shift [13].

Figure 2 presents the energy and potential as a function of inter-cluster distance in the  $\alpha$ - $\alpha$  system. The  $\alpha$ - $\alpha$  system is represented by the Brink-type wave function. Namely, two  $\alpha$  clusters are located at points,  $(x, y, z) = (0, 0, d/2)$  and  $(x, y, z) = (0, 0, -d/2)$ , where  $d$  indicates the inter-cluster distance. The width parameter of an  $\alpha$  is fixed to be  $\nu = 0.25 \text{ fm}^{-2}$ . All of the energy curves have minimum points at around  $d \sim 3 \text{ fm}$ . The energy and potential for F3B force and for Volkov No.2( $m = 0.60$ ) are very similar to each other in the region  $d > 2.5 \text{ fm}$ . In the small-distance region  $d < 2 \text{ fm}$ , the  $\alpha$ - $\alpha$  potential in the case of the F3B force is shallower than that for Volkov No.2 because of the three-body repulsive term. The  $\alpha$ - $\alpha$  potential for the Gogny D1 force and the MV1 case(1) force( $m = 0.60$ ) are similar to each other. Both forces indicate a smaller inter-cluster potential compared with the Volkov No.2 ( $m = 0.60$ ) force. This result is consistent with the  $\alpha$ - $\alpha$  scattering behavior.

#### B. $^{16}\text{O}$ - $\alpha$ system

The total and potential energy of the  $^{16}\text{O}$ - $\alpha$  system is shown in Fig. 3 and Fig. 4. The  $^{16}\text{O}$ - $\alpha$  system is represented by the Brink-type wave function. Namely,  $^{16}\text{O}$  and  $\alpha$  described by the harmonic oscillator wave functions are located at  $(x, y, z) = (0, 0, d/5)$  and  $(x, y, z) = (0, 0, -4d/5)$ , where  $d$  is the inter-cluster distance. The intrinsic energy of clusters is subtracted. The width parameter of  $^{16}\text{O}$  and  $\alpha$  is chosen to be the optimum width which gives the minimum energy of  $^{20}\text{Ne}$  for each forces. As shown in Fig. 3, the potential energy is similar among three forces(Gogny, MV1

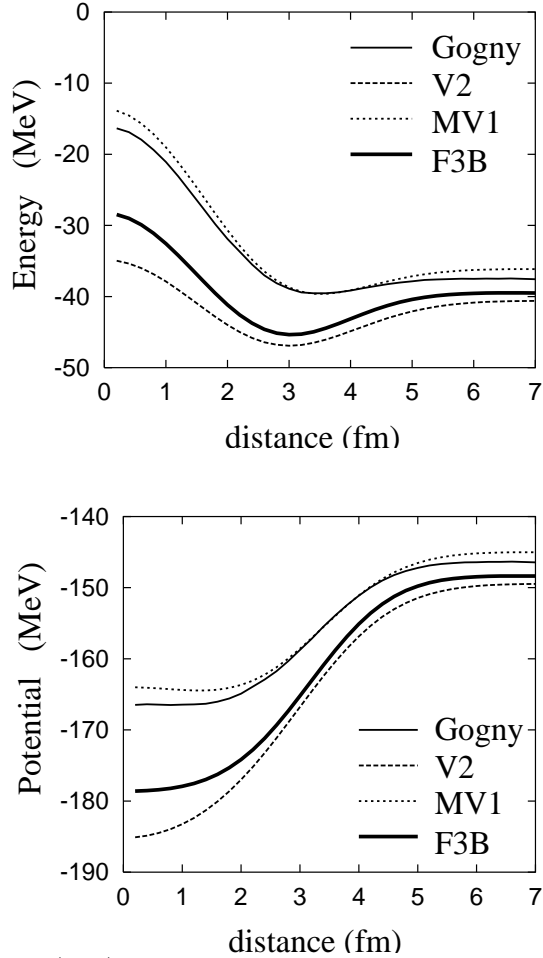


FIG. 2. Energy and potential between  ${}^4\text{He}$ - ${}^4\text{He}$ . The potential energy(total energy) of the  ${}^4\text{He}$ - ${}^4\text{He}$  system as functions of the relative distance ( $d$ ) is shown in the lower(upper) panel. The effective forces are Gogny D1, Volkov( $m = 0.60$ ), MV1 cases 1( $m = 0.60$ ) and F3B.

TABLE II. The binding energy of the band head states( $0_1^+$  and  $1_1^-$ ) of the parity doublets in  ${}^{20}\text{Ne}$  calculated with the AMD+GCM method. The adopted Hamiltonian is same as Eq.8. The F3B case(1) and the MV3 case 1( $m = 0.60$ ) are used as the central forces. The width parameter is chosen to be  $\nu = 0.20$  and  $\nu = 0.165$ , which minimise the binding energy of  ${}^{20}\text{Ne}$ , for the F3B case(1) and MV3 case 1( $m = 0.60$ ) forces, respectively. Excitation energy of the  $1_1^-$  states are also shown.

(MeV)	F3B	MV3	exp.
$0_1^+$	157.2	153.1	160.647
$1_1^-$	151.4	146.5	154.859
$E_x(1_1^-)$	5.8	6.5	5.788

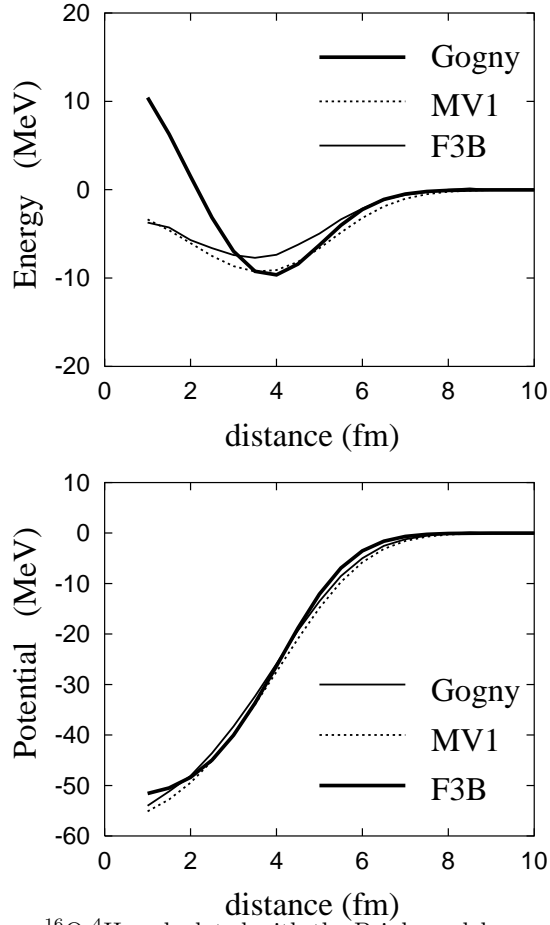


FIG. 3. Energy and potential between  $^{16}\text{O}$ - $^4\text{He}$  calculated with the Brink model wave functions. The potential energy (total energy) of the  $^{16}\text{O}$ - $^4\text{He}$  system as functions of the relative distance  $d$  is shown in the lower (upper) panel. The effective forces are Gogny D1, MV1 case 1 ( $m = 0.60$ ) and F3B forces. Width parameters are chosen to be optimum widths which give the minimum energy for  $^{20}\text{Ne}$ , i.e.  $\nu = 0.16, \nu = 0.165$  and  $\nu = 0.20$  for the Gogny D1, MV1 case 1 ( $m = 0.60$ ) and F3B forces, respectively.

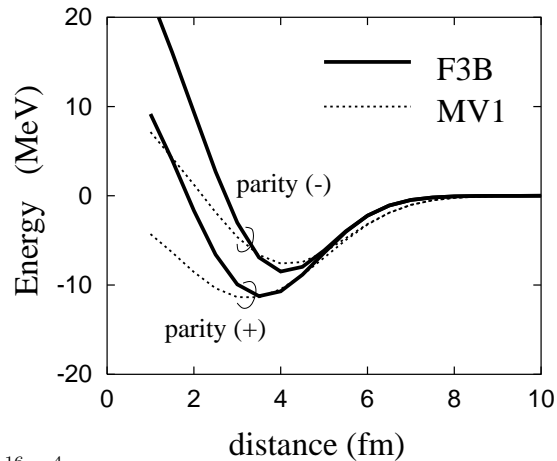


FIG. 4. The total energy of the  $^{16}\text{O}$ - $^4\text{He}$  system for the parity-projected states calculated with the Brink model wave functions.  $d$  is the relative distance between  $^{16}\text{O}$  and  $^4\text{He}$ . Width parameters are chosen to be optimum widths which give the minimum energy for  $^{20}\text{Ne}$ , i.e.  $\nu = 0.165$  and  $\nu = 0.20$  for the MV1 case 1 ( $m = 0.60$ ) and F3B forces, respectively.

case 1( $m = 0.60$ ) and F3B). In the total energy (Fig.3), the minimum energy points exist at almost the same distance  $d \sim 4$  fm for the MV1 case 1( $m = 0.60$ ) and F3B forces. In the small distance region, the F3B force has a more repulsive term of the total energy than the MV1 case 1( $m = 0.60$ ) force because the width parameter  $nu$  is larger for the F3B force than the MV1 case 1( $m = 0.60$ ) force, therefore, the kinetic energy increases more rapidly as the inter-cluster distance become small.

The  $^{16}\text{O}-\alpha$  potential energy is closely related to the structure of parity doublet states in  $^{20}\text{Ne}$ . The  $K = 0_1^+$  and the  $K = 0_1^-$  bands in  $^{20}\text{Ne}$  are known to be the parity doublet states, which are considered to originate from the  $^{16}\text{O}+\alpha$  cluster structure. In Fig. 4, the total energy of the parity-projected states for the Brink-type wave functions are plotted as a function of the inter-cluster distance  $d$ . Comparing the results with the F3B force and MV1 force, the minimum energy is qualitatively similar. The minimum energy point for the positive-parity states shifts to the large distance region in case of the F3B force, which has an effect on the enhancement of the  $^{16}\text{O}+\alpha$  clustering in  $^{20}\text{Ne}$ .

In the above-mentioned discussion, the  $^{16}\text{O}-\alpha$  potential are studied within the framework, where the  $^{16}\text{O}$  and  $\alpha$  are treated as inert clusters written by harmonic oscillator wave functions. However, in the real  $^{20}\text{Ne}$ , the core excitation is more important than the case of  $\alpha-\alpha$  system. Moreover, the harmonic oscillator wave function is too simple to describe the real  $^{16}\text{O}$  nucleus. In order to see agreements to the experimental data, we calculate the band-head states( $0_1^+$  and  $1_1^-$ ) of the parity doublets in  $^{20}\text{Ne}$  with the AMD+GCM method, where the effect of core excitation is automatically included. The detailed description of the method is given later. As shown in Table II, the binding energy and the excitation energy of the  $1_1^-$  state are well reproduced by using the F3B force.

### C. Radii and Binding energy of $Z = N (A \leq 40)$ nuclei and O isotopes

In order to discuss the features of the saturation properties (radii and binding energy) in finite nuclei, we apply the F3B forces to microscopic calculations based on a AMD method for  $Z = N (A \leq 40)$  nuclei and O isotopes.  $\nu = 0.16$ . The formulation of AMD for a nuclear structure study of ground and excited states is explained in [1,2,17]. Here, we briefly explain the framework in the present work, namely, the generator coordinate method in the framework of AMD with constraint (AMD+GCM). The wave function of a system is written by superposition of AMD wave functions,

$$\Phi = c\Phi_{AMD} + c'\Phi'_{AMD} + \dots \quad (5)$$

An AMD wave function of a nucleus with mass number  $A$  is a Slater determinant of Gaussian wave packets:

$$\Phi_{AMD}(\mathbf{Z}) = \frac{1}{\sqrt{A!}} \mathcal{A}\{\varphi_1, \varphi_2, \dots, \varphi_A\}, \quad (6)$$

$$\varphi_i = \phi_{\mathbf{X}_i} \chi_{\xi_i} \chi_{\tau_i} : \begin{cases} \phi_{\mathbf{X}_i}(\mathbf{r}_j) \propto \exp[-\nu(\mathbf{r}_j - \frac{\mathbf{X}_i}{\sqrt{\nu}})^2], \\ \chi_{\xi_i} = \begin{pmatrix} \frac{1}{2} + \xi_i \\ \frac{1}{2} - \xi_i \end{pmatrix}, \end{cases} \quad (7)$$

where the  $i$ th single-particle wave function ( $\varphi_i$ ) is a product of the spatial wave function ( $\phi_{\mathbf{X}_i}$ ), the intrinsic spin function ( $\chi_{\xi_i}$ ) and the iso-spin function ( $\chi_{\tau_i}$ ). The spatial part ( $\phi_{\mathbf{X}_i}$ ) is represented by complex variational parameters( $X_{1i}$ ,  $X_{2i}$ ,  $X_{3i}$ ).  $\chi_{\xi_i}$  is the intrinsic spin function, defined by  $\xi_i$ , and  $\tau_i$  is an iso-spin function, which was fixed to be up(proton) or down(neutron) in the present calculations. Thus, an AMD wave function is expressed by a set of variational parameters,  $\mathbf{Z} \equiv \{X_{ni}, \xi_i\}$  ( $n = 1, 2, 3$  and  $i = 1, \dots, A$ ), which stand for the centers of Gaussians of the spatial part and the intrinsic spin orientations of the single-particle wave functions. By using the frictional cooling method, we performed energy variation with respect to a parity-projected AMD wave function,  $\Phi^\pm$ , while satisfying the condition that the principal oscillator quantum number of the system,  $\langle a^\dagger a \rangle \equiv \langle \Phi^\pm | \sum_i^A \hat{\mathbf{a}}_i^\dagger \cdot \hat{\mathbf{a}}_i | \Phi^\pm \rangle / \langle \Phi^\pm | \Phi^\pm \rangle$ , equals a given number. After variation with the constraint on the oscillator quanta, we superposed the spin-parity eigen states projected from the obtained AMD wave functions so as to diagonalize the Hamiltonian matrix and the norm matrix. The expectation values for such structure properties as the binding energy and the root-mean-square radius were evaluated by the superpositions. In the present calculations, we superposed several spin-parity projected AMD wave functions with respect to the generator coordinate,  $\langle a^\dagger a \rangle$ .

The used Hamiltonian in the AMD+GCM calculations was,

$$\mathcal{H} = -\frac{\hbar^2}{2M} \sum_i \nabla_i^2 - T_G + V_{coulomb} + V_{central} + V_{spin-orbit}, \quad (8)$$

where the first term stands for the kinetic energy operator, the second is for extraction of the center of mass energy, and  $V_{coulomb}$  means the Coulomb energy term. The central force,  $V_{central}$ , is the F3B force. In addition to the central force, we employ the following two-body spin-orbit force( $V_{spin-orbit}$ ) :

TABLE III. Calculated binding energy and root-mean-square radii for a point-like proton distribution. Theoretical values for the F3B case (1) were obtained by AMD+GCM calculations. The values with the Volkov force No.2(V2), A modified Volkov force(MV1) case 1 and Tohsaki’s F1 force are those calculated by the closed-shell HO wave functions ([12,13]). The center-of-mass correction in the theoretical radii for V2, MV1, Tohsaki’s F1 forces is subtracted as  $\langle r^2 \rangle - 3/2aA$  ( $A$  is the mass number and  $a$  is the harmonic oscillator size parameter related to  $\hbar\omega = \hbar^2a/M$ , where  $M$  is the nucleon mass.) The theoretical values of the Skyrme III force are three-dimensional HF+BCS calculations by N. Tajima et al [5]. The value in parenthesis was calculated with a single AMD wave function (the values for SIII are taken from [19]). The experimental r.m.s.r. were deduced from the charge radii [20].

	Force	V2( $m = 0.65$ )	MV1(case1)	SIII	Tohsaki’s F1	F3B(this work)	exp.
$^4\text{He}$	$E(\text{MeV})$	28.0	28.2	26.5(25.6)	27.5	28.2(28.0)	28.296
	r.m.s.r.(fm)	1.46	1.64	1.88(1.66)	1.50	1.52(1.48)	1.47
$^{16}\text{O}$	$E(\text{MeV})$	105.9	122.2	128.1(120.9)	123.0	129.7	127.617
	r.m.s.r.(fm)	2.35	2.62	2.63(2.60)	2.48	2.57	2.57
$^{40}\text{Ca}$	$E(\text{MeV})$	348	351.6	341.8	334.0	350.6	342.046
	r.m.s.r.(fm)	2.64	3.31	3.40	3.38	3.38	3.39

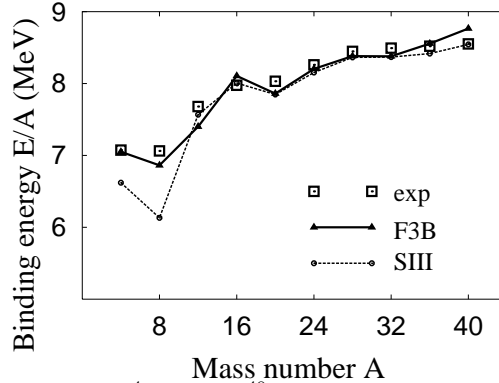


FIG. 5. Binding energy of  $Z = N$  nuclei from  $^4\text{He}$  up to  $^{40}\text{Ca}$ , calculated by AMD+GCM with the F3B case (1) compared with the experimental data. The theoretical values by HF+BCS calculations with SIII [5] are also displayed.

$$V_{spin-orbit} = \sum_{i < j} V^{(LS)}, \quad (9)$$

$$V_{ij}^{(LS)} = \frac{1+P_\sigma}{2} \frac{1+P_\tau}{2} \mathbf{1}_{ij} \cdot \mathbf{s}_{ij} \sum_{n=1}^2 \left\{ v_n^{(LS)} \exp \left[ -\left( \frac{\mathbf{r}_i - \mathbf{r}_j}{a_n^{(LS)}} \right)^2 \right] \right\}, \quad (10)$$

where the same range of parameters as those of the G3RS force [18],  $a_1^{(LS)} = 0.4472$  fm and  $a_2^{(LS)} = 0.5774$  fm, are used. The strengths of the spin-orbit force were chosen to be  $v_1^{(LS)} = -v_2^{(LS)} = 1800$  MeV in the present calculations.

In Table III, the results of root-mean-square radii (r.m.s.r) for point-like proton distributions of double-closed nuclei,  $^4\text{He}$ ,  $^{16}\text{O}$  and  $^{40}\text{Ca}$  are listed. It is found that, overall, the F3B force well reproduces the radii and energy of these nuclei as well as Tohsaki’s F1 force. It has been already known that it is impossible to systematically describe the nuclear saturation properties by Volkov forces. For instance, in the case of Volkov No.2(V2) with the Majorana exchange parameter  $m = 0.65$ , the radii of  $^{16}\text{O}$  and  $^{40}\text{Ca}$  are largely underestimated. On the other hand, the MV1 force and the SIII force fail to qualitatively reproduce the compact size of a real  $^4\text{He}$ . A HF+BCS calculation with SIII gives an extremely large radius of an  $\alpha$  particle because the center-of-mass motion is not exactly extracted in the model space. By an AMD calculation, where the center-of-mass motion was microscopically extracted, the calculated  $\alpha$  radius with the SIII force was found to be 1.66 fm, which is as large as those with the MV1 force and the SIII force. Therefore, we can conclude that these forces with zero-range density-dependent terms always overestimate the correct size of an  $\alpha$  particle.

In Figs. 5 and 6, the present results of the binding energy and the proton r.m.s.r. of  $Z = N$  nuclei up to  $^{40}\text{Ca}$  with the F3B forces are compared with the experimental data. The present results well agree with the overall data in this nuclear region.

Although the parameter sets, case (1) and case (2), of the F3B force give almost the same results for  $Z = N$  nuclei, the results for  $Z \neq N$  nuclei are different because the ratios of the inter-nucleon interaction for the isospin



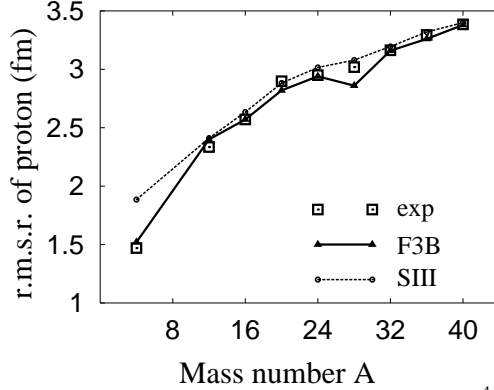


FIG. 6. Root-mean-square radii of the proton density for  $Z = N$  nuclei from  ${}^4\text{He}$  up to  ${}^{40}\text{Ca}$  calculated by AMD+GCM with the F3B case (1). The experimental data were deduced from the charge r.m.s.r. [20]. The theoretical values by HF+BCS with SIII [5] are also shown.

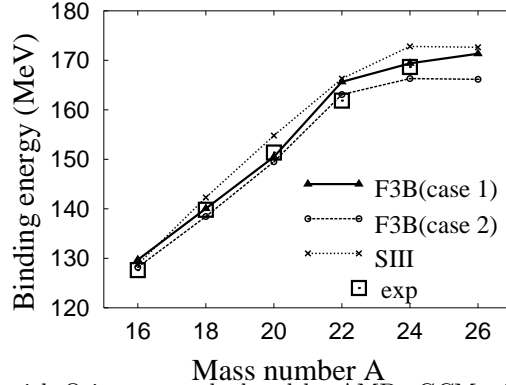


FIG. 7. Binding energy of neutron-rich O isotopes calculated by AMD+GCM with F3B case 1 and case 2. The HF+BCS calculations with SIII [5] and the experimental data are also displayed.

$T = 1$  system to that for the  $T = 0$  system are different between cases (1) and (2). The theoretical binding energy of neutron-rich O isotopes are compared with the experimental data in Fig. 7. The calculated results with both sets of interaction parameters agree reasonably with the experimental data.  ${}^{26}\text{O}$  is known to be a particle-unstable nucleus. Concerning the systematics of the two-neutron separation energy, the neutron drip line in O isotopes is reproduced by the case (2) force. Although the drip line is not described by the case (1) force, we can not conclude that the parameter case (1) is inappropriate at the present stage because the present model space seems to be insufficient to describe the detailed structure of  ${}^{24}\text{O}$ , as conjectured from a disagreement between the theoretical radius and the experimental one.

The present results concerning the r.m.s.r of O isotopes quantitatively agree with the experimental data deduced from the interaction cross-section data [21], except for  ${}^{24}\text{O}$  (Fig. 8). The reason for the failure in reproducing the enhancement of the radius near to the drip line is conjectured that the present model space is not sufficient to describe the detailed behaviour of weakly bound neutrons.

#### D. nuclear matter property

The matter properties were evaluated by plane waves in the Fermi sea. The equation of state(EOS) of the symmetric nuclear matter is illustrated in Fig. 9. The properties at the saturation point are listed in Table IV. The SIII force, Gogny D1 force, Tohsaki's F1 force, F3B force give similar results for the saturation energy  $E_s/A$  and the saturation density  $\rho_s$  ( $\rho_s = 2k_f^3/3\pi^2$ , where  $k_f$  is Fermi momentum at the saturation point). On the other hand, the MV1 force can not satisfactorily explain the following empirical values:  $E_s/A \sim -16$  MeV and  $\rho_s \sim 0.16$  fm $^{-3}$  ( $k_f \sim 1.33$  fm $^{-1}$ ).

The small incompressibility of matter( $K_\infty$ ), namely, the soft-type equation of state(EOS) is given by such effective forces as the Gogny force and the SLy4 forces(a Skyrme parametrization) [11], while the F3B, SIII, Tohsaki's F1,

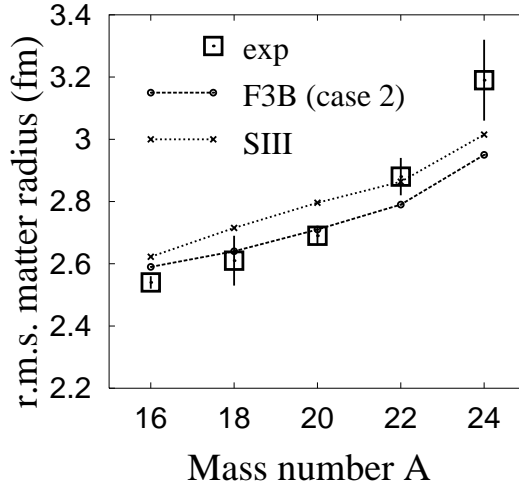


FIG. 8. Root-mean-square(r.m.s.) matter radii calculated by AMD+GCM with F3B case 2. The experimental data are those deduced from the reaction cross sections taken from Ref. [21]. The theoretical values by HF+BCS with SIII [5] are also shown.

MV1 forces give large values of incompressibility, which correspond to the hard EOS (see table IV). Comparing EOS for the F3B force with that for the Gogny D1 force, it is found that the EOS is similar to each other in the low-density region, while the matter energy for the F3B force rapidly increases in the high-density region. The incompressibility of nuclear matter has been discussed in relation to the energy of giant monopole resonances(GMR) [22–25]. Although a soft-type equation of state(EOS), like  $K_\infty = 200 \sim 240$ , is preferred to quantitatively describe the GMR energy in HF analysis with Gogny and Skyrms-type effective forces [23,22], there still remains an inconsistency with the theoretical values suggested by a relativistic-mean-field analysis [25], where larger incompressibilities are predicted. On the other hand, the hard-type Tohsaki’s F1 force reasonably reproduces the GMR energy of  $^{40}\text{Ca}$  [13].

It has been known that matter saturation can not be described by effective two-body central forces without any repulsive density-dependent or three-body terms, as can be seen in the EOS given by the Volkov force (Fig. 9). In other words, the density-dependent or three-body terms are essential to explain the nuclear matter saturation. In order to exhibit the mechanism of nuclear saturation, we decomposed the total potential energy into different contributions,  $E^{(ST)}$ , in each subspace ( $ST$ ), defined by the projectors  $P^{(ST)} = (1 \pm P_\sigma)(1 \pm P_\tau)/4$  in the same way as is the analysis described in Ref. [9]. The decomposed potential energy of the F3B forces is shown in Fig. 10. The dominant parts of the potential energy at a saturation density of  $k_f \sim 1.3 \text{ fm}^{-1}$  are the singlet even( $^1E$ ) and triplet even( $^3E$ ) terms, while the singlet odd ( $^1O$ ) and triplet odd ( $^3O$ ) parts are minor. We notice that the  $^3E$  part plays an important role in the saturation mechanism. This result is consistent with a tendency which was indicated in the nuclear matter calculations by Brueckner-Goldstone Theory using realistic nucleon-nucleon interactions [26]. It is very reasonable because the matter saturation is considered to come from a suppression of the tensor part of the bare nucleon-nucleon interaction in nuclear matter, because the Pauli principle acts to reduce the attractive tensor force due to a blocking of the intermediate states. Therefore, tensor suppression in nuclear matter is regarded to be phenomenologically simulated by the repulsive density-dependent terms in the effective central forces. In that sense, the repulsive density-dependent term should be dominated by the triplet even component, just as in the case of the tensor force. As a result, the triplet even component indicates the saturation behavior with an increase of density. Strictly speaking, also, the  $^3O$  part of the potential energy has an enhancement in the region  $k_f \geq 1.5 \text{ fm}^{-1}$ , because the three-body repulsive term is not pure  $^3E$ , but it also contains the  $^3O$  component because of the simple form of the three-body operator in F3B forces. Such an enhancement in a rather high-density region may have at least no significant effect on the structure of finite nuclei.

## IV. DISCUSSION

### A. Significance of finite-range three-body term

The finite-range three-body terms in the phenomenological effective forces are important to describe the overall properties for nuclei for a broad range of masses. As mentioned in III, and also already argued in the pioneering work

TABLE IV. Saturation Properties for nuclear matter. The saturation energy, Fermi momentum, and incompressibility at the saturation point for various effective forces.

Force	MV1(case1 $m=0.60$ )	SIII	SLy4	Gogny(D1)	Tohsaki's F1	F3B(this work)
$E/A(\text{MeV})$	-21.01	-15.87	-15.97	-16.32	-17.0	-17.9
$k_f(\text{fm}^{-1})$	1.48	1.29	1.33	1.35	1.27	1.32
$K_\infty(\text{MeV})$	299	356	230	228	309	390

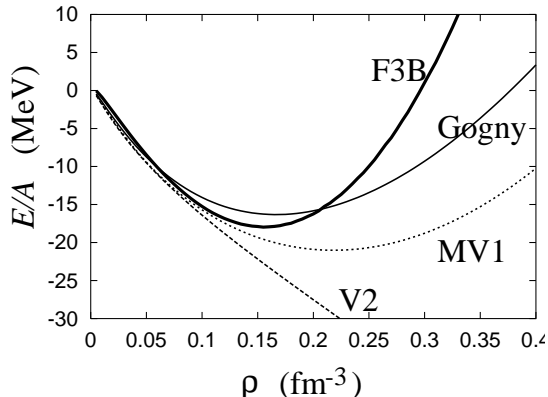


FIG. 9. Equation of state for symmetric nuclear matter. The energy per nucleon is plotted as a function of the density. The effective forces are Gogny D1, F3B, Volkov No.2( $m = 0.65$ ), and MV1 case 1( $m = 0.60$ ).

by Tohsaki [13], the finite-range three-body terms are empirically essential to simultaneously reproduce the properties of  $\alpha$ -particle(size and  $\alpha$ - $\alpha$  phase shift) and nuclear matter saturation. Moreover, the finite-range feature is reasonable considering the original range of the tensor force, whose suppression effect in matter is simulated by the three-body terms. In order to explain the indispensability of the finite-range nature in three-body terms, we demonstrate the fatal failure of general effective forces with zero-range density-dependent terms in describing the correct size and energy of an  $\alpha$  particle and the saturation density and energy of nuclear matter. We assume an effective central force, which consists of a two-body term with a two-range Gaussian form and a zero-range density-dependent term, as follows:

$$V_{ij} = (1 - m - mP_\sigma P_\tau) \left[ v_1 \exp\left(-\frac{r_{ij}^2}{a_1^2}\right) + v_2 \exp\left(-\frac{r_{ij}^2}{a_2^2}\right) \right] + v_3 \rho^\sigma(r_{ij}) \cdot \delta(r_{ij}), \quad (11)$$

$$\text{where} \quad \sigma = \frac{1}{3} \text{ or } 1. \quad (12)$$

Coulomb force is omitted. By assuming the  $(0s)^4$  HO wave function for an  $\alpha$  particle and plane waves in the Fermi sea for nuclear matter, we can easily obtain the optimum size( $r_\alpha$ ) and energy( $E_\alpha$ ) of an  $\alpha$  particle and the matter saturation density( $\rho_s$ ) and energy( $E_s$ ) as a function of the parameter set  $(v_1, a_1, v_2, a_2, v_3, m)$  as  $r_\alpha(v_1, a_1, v_2, a_2, v_3, m)$ ,  $E_\alpha(v_1, a_1, v_2, a_2, v_3, m)$ ,  $\rho_s(v_1, a_1, v_2, a_2, v_3, m)$ , and  $E_s(v_1, a_1, v_2, a_2, v_3, m)/A$ . We try to search for a parameter set which can reproduce the empirical data of these four values. Firstly, we put the following conditions: that the size and energy of an  $\alpha$  particle are equal to the experimental data,  $r_\alpha = 1.48$  fm and  $E_\alpha = 29.253$  MeV. Here, the experimental input of the energy is a modified one with a Coulomb-force correction. Keeping these two constraints, we vary the parameters  $(v_1, a_1, v_2, a_2, v_3, m)$  in the following ranges:  $0.6 \leq a_1 \leq 2.5$  fm,  $0.5 \leq a_2 \leq a_1$  fm,  $100 \leq v_3 \leq 4000$  MeV fm<sup>4</sup>( $\sigma = 1/3$ ) or  $100 \leq v_3 \leq 4000$  MeV fm<sup>6</sup>( $\sigma = 1$ ),  $0.01 \leq m \leq 0.99$ , and investigate the behaviour of the matter saturation point  $(\rho_s, E_s/A)$ , given by the various sets of paramters. We also put a physical restriction,  $v_1 \leq 0$ , that indicates that the long-range term must be attractive. The saturation points  $(\rho_s, E_s/A)$  are displayed in Fig. 11. The upper panel indicates the saturation points in the case  $\sigma = 1/3$ , and the lower panel corresponds to the case  $\sigma = 1$ . Under the conditions of the  $\alpha$ -particle properties, the saturation points can not reach the empirical saturation point ( $\rho_s \sim 0.16$  fm<sup>-3</sup>,  $E_s/A \sim -16$  MeV) in both cases, because the allowed area of the saturation points does not include the empirical one. This means that there is no reasonable parameter set which is able to simultaneously describe the saturation properties of an  $\alpha$  particle and nuclear matter. In other words, with “zero-range” density-dependent-type effective central forces, which explain the matter saturation point, it is difficult to describe the compact size of a real  $\alpha$  particle. From these results, we can conclude that the finite-range terms are indispensable to simultaneously reproduce the properties of  $\alpha$ -particle and matter saturation.

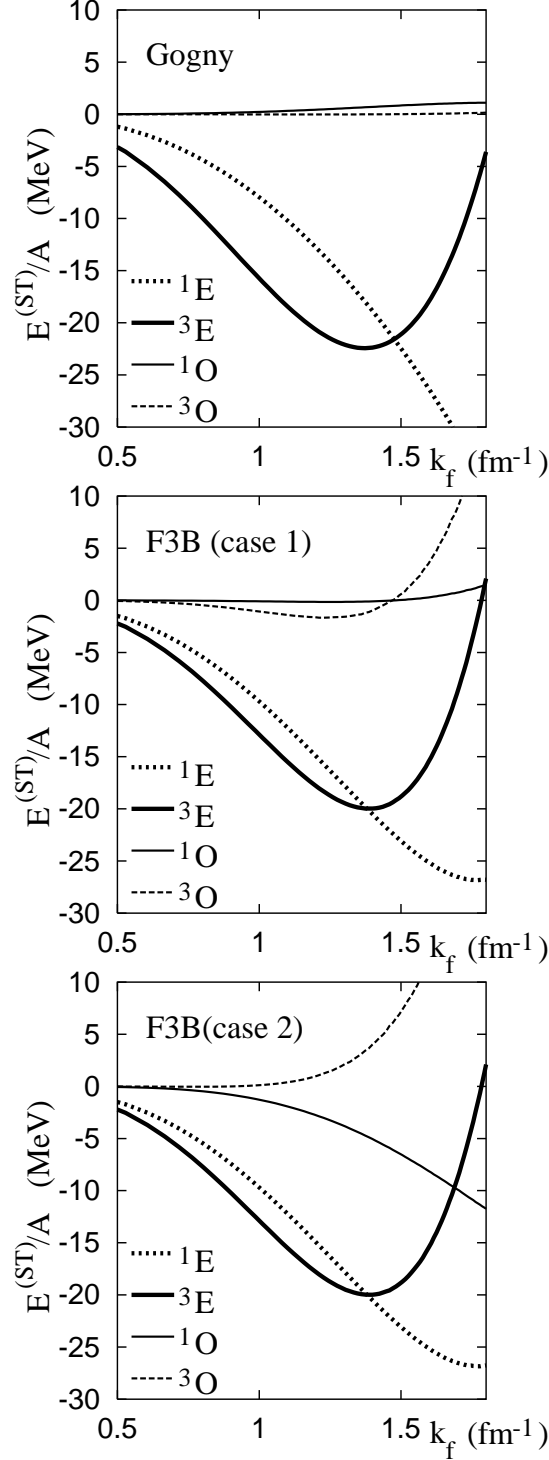


FIG. 10. Partial contributions  $E^{(ST)}$  of the potential energy in each subspace of singlet even( $^1E$ ), triplet even( $^3E$ ), singlet odd( $^1O$ ) and triplet odd( $^3O$ ) defined by the projectors  $P^{(ST)} = (1 \pm P_\sigma)(1 \pm P_\tau)/4$ , where  $(ST)=(0,1)$ ,  $(1,0)$ ,  $(0,0)$  and  $(1,1)$ , respectively. The calculated values of the partial potential energy per nucleon are plotted as functions of the Fermi momentum( $k_f$ ).

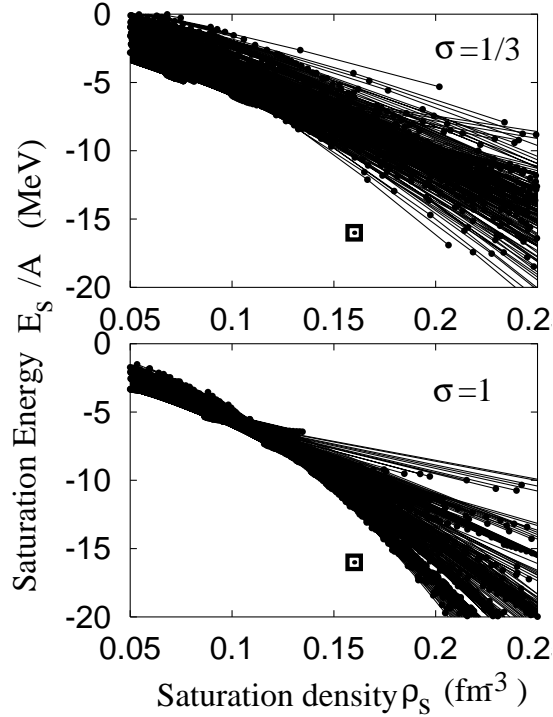


FIG. 11. Dots indicate the saturation energy and density in symmetric nuclear matter obtained by effective central forces with finite-range two-body terms and a zero-range density-dependent term, which satisfy the experimental data of the size and energy of an  $\alpha$  particle. The square points correspond to the empirical saturation energy and density ( $\rho_s = 0.16 \text{ fm}^{-3}$ ,  $E_s/A = -16 \text{ MeV}$ ). The details are explained in the text.

### B. Relation with $s$ -wave nucleon-nucleon scattering

It has already been known that bare nucleon-nucleon interactions have leading tensor terms and hard cores, both of which are not easily treated in the microscopic calculations of nuclear many-body systems. Instead, one usually adopts phenomenological effective nucleon-nucleon forces dominated by central forces with no hard cores. It is regarded that the tensor terms and hard cores are renormalized in the effective central forces. As already mentioned, the necessity of repulsive density-dependent terms of effective forces for describing the saturation properties originates from a suppression of the attractive tensor force in nuclear matter [26]. In other words, the density dependence of the tensor force suppression is phenomenologically simulated by density-dependent repulsive terms in the effective central forces. From this point of view, we demonstrate a link between the effective forces and nucleon-nucleon(N-N) scattering and discuss the role of the density-dependent repulsive terms. Firstly, we reproduce the  $s$ -wave N-N scattering phase shift by the central two-body forces in the F3B force. Second, we discuss the role of the residual part with the three-body term, which should be connected with the matter effect on the N-N interaction.

We decompose the central part of the present effective force(F3B) into two terms. One is a two-body term,  $V^{2\text{-body}}$ , which can reproduce the  $s$ -wave nucleon-nucleon scattering behaviour, and the other is the residual term,  $\Delta V$ , which contains the three-body term, defined as follows:

$$V_{\text{central}} = \sum_{i<j} V_{ij}^{(2)} + \sum_{i<j<k} V_{ijk}^{(3)} = V^{2\text{-body}} + \Delta V, \quad (13)$$

$$V^{2\text{-body}} = \sum_{i<j} V_{ij}^{(2)} + \sum_{i<j} V'_{ij}, \quad (14)$$

$$\Delta V = -\sum_{i<j} V'_{ij} + \sum_{i<j<k} V_{ijk}^{(3)} \quad (15)$$

$$, \quad V'_{ij} = v' \exp \left[ -\left( \frac{\mathbf{r}_i - \mathbf{r}_j}{a_3^{(2)}} \right)^2 \right], \quad (16)$$

where  $v' = 32.5 \text{ MeV}$ . Other interaction parameters in  $V_{ij}^{(2)}$  and  $V_{ijk}^{(3)}$  are same as those of F3B force. The first term  $V^{2\text{-body}}$  in Eq. 13 is the two-body central force. The  $s$ -wave phase shift for the low-energy N-N scattering data is well described by this two-body term  $V^{2\text{-body}}$ , as shown in Fig. 12. Moreover, the calculated scattering lengths of

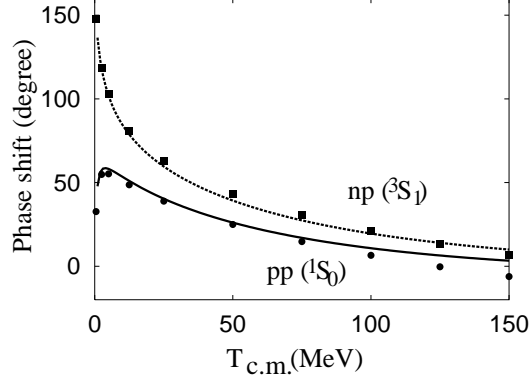


FIG. 12.  $s$ -wave phase shift of nucleon-nucleon scattering calculated with the effective two-body central force  $V^{2\text{-body}}$  defined in equations 13-16 of the text.

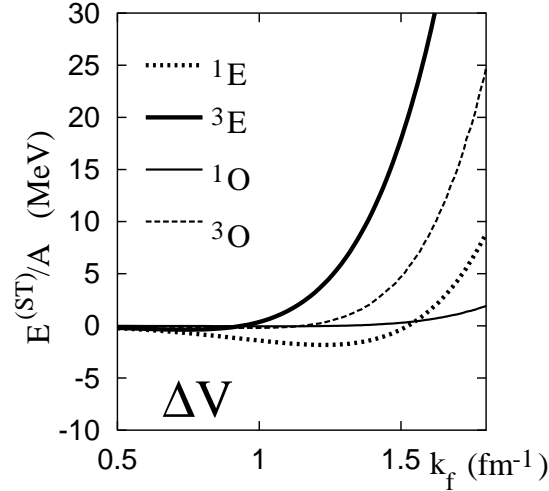


FIG. 13. Partial contributions  $E^{(ST)}$  of the nuclear matter potential energy for  $\Delta V$  in each subspace defined by the projectors  $P^{(ST)} = (1 \pm P_\sigma)(1 \pm P_\tau)/4$ .

the singlet and triplet  $s$ -wave for  $V^{2\text{-body}}$  are  $a_s = 5.37(\text{fm})$  and  $a_t = -19.6(\text{fm})$ , which reasonably agree with the experimental values,  $a_s = 5.39$  and  $a_t = -23.7$ . Therefore, we consider this  $V^{2\text{-body}}$  as an effective force between bare nucleons, where the tensor force in the realistic interaction is renormalized in the central term. Thus, the second term( $\Delta V$ ) in Eq. 13 can be understood in terms of the matter effect in finite nuclei and nuclear matter. Since the leading matter effect originates from a suppression of the tensor force,  $\Delta V$  should be repulsive, and behaves as triplet even. In Fig. 13, we represent the partial contributions,  $E^{(ST)}$ , of the potential energy given by  $\Delta V$  in each subspace ( $ST$ ) of nuclear matter. At a saturation density of  $k_f \sim 1.3 \text{ fm}^{-1}$ , the dominant component of  $\Delta V$  is the triplet even part. This means that the density-dependent repulsive term( $\Delta V$ ) actually takes the role of tensor force suppression in nuclear matter.

As mentioned above, the central effective force(F3B) is decomposed into two parts,  $V^{2\text{-body}}$  and  $\Delta V$ . In principle, it is easy to understand the decomposition if  $V^{2\text{-body}}$  is same as the two-body term  $\sum_{i<j} V_{ij}^{(2)}$  of the F3B force, and  $\Delta V$  consists of only the three-body term of F3B. However, in the present analysis,  $V^{2\text{-body}}$  is the modified one from the original  $\sum_{i<j} V_{ij}^{(2)}$ , and  $\Delta V$  involves a two-body term in addition to the dominant three-body term. We consider the reason as following way. The origin of the finite-range three-body term may not be the pure three-body effect but it also contains some component from the two-body central force. It is because of the restriction of the simple finite-range three-body operator, where we adopt a common range for the distances of all nucleon pairs in three-body term and omit spin-dependent terms for simplicity to apply to practical calculations with AMD method. In order to overcome the restriction, we consider that  $\Delta V$ , which consists of the two-body and three-body terms, indicates the matter effect and means the effective density-dependent repulsive force.

## V. SUMMARY

We proposed new effective inter-nucleon forces with a finite-range three-body operator for microscopic calculations of nuclear structure. It was found that the proposed forces are suitable to describe saturation properties over a wide mass number region from the  $\alpha$  particle to nuclear matter. Compared with similar-type forces proposed by Tohsaki, an advantage of the new forces is that they are more practical because of the simple three-body operator, and therefore are applicable to microscopic calculations of general nuclei. The proposed effective forces were applied to AMD+GCM calculations of  $Z = N$  ( $A \leq 40$ ) nuclei and O isotopes. In addition to the success in systematically reproducing the radii and energy of these nuclei, we demonstrated the characteristics of the new forces concerning the  $\alpha$ - $\alpha$  scattering behaviour and matter EOS. Especially, the new forces successfully describe the compact size of a real  $\alpha$  particle and the  $\alpha$ - $\alpha$  scattering phase shift, which typical effective forces with zero-range density-dependent terms can not reproduce. Concerning the matter properties, we found that the saturation mechanism in the nuclear matter originates from the dominant triplet even component in the repulsive three-body term. The new forces were also discussed in relation with the  $s$ -wave N-N scattering behavior.

The density-dependent repulsive terms are essential to describe nuclear saturation. The origin is a suppression of the tensor force of bare nucleon-nucleon interactions in nuclear matter. From this point of view, we discussed the role of the finite-range three-body term in the new forces. The importance of the finite-range three-body term was also described based on empirical concepts. We conclude that the finite-range three-body operator plays an essential role in describing the overall properties over a wide mass number region as well as the matter saturation properties.

## ACKNOWLEDGMENTS

The authors would like to thank Dr. A. Ono, Prof. A. Tohsaki and Prof. H. Horiuchi and Prof. K. Ikeda for helpful discussions and comments. They are thankful to Dr. O. Morimatsu and Dr. H. Nemura for technical advise. A part of the calculations were performed with the AMD code(version 2.5) provided by Dr. A. Ono. The computational calculations of this work were supported by the Supercomputer Project No.58, No.70 and No.83 of High Energy Accelerator Research Organization(KEK), and Research Center for Nuclear Physics in Osaka University. This work was supported by Japan Society for the Promotion of Science and a Grant-in-Aid for Scientific Research of the Japan Ministry of Education, Science and Culture. The work was partially performed in the “Research Project for Study of Unstable Nuclei from Nuclear Cluster Aspects” sponsored by Institute of Physical and Chemical Research (RIKEN).

- 
- [1] Y. Kanada-En'yo, M. Kimura and H. Horiuchi, *Comptes rendus Physique* Vol.4, 497(2003).
  - [2] Y. Kanada-En'yo, H. Horiuchi and A. Ono, *Phys. Rev. C* **52**, 628 (1995); Y. Kanada-En'yo and H. Horiuchi, *Phys. Rev. C* **52**, 647 (1995).
  - [3] Y. Kanada-En'yo and H. Horiuchi, *Prog. Theor. Phys. Suppl.* **142**, 205(2001).
  - [4] P. Bonche et al., *Nucl. Phys.* **A443**, 39 (1985).
  - [5] N.Tajima, S.Takahara and N.Onishi, *Nucl.Phys.* **A603**, 23 (1996).
  - [6] S.Takami, K.Yabana and K.Ikeda, *Prog.Theor.Phys.* **96**, 407 (1996).
  - [7] D. R. Thompson, M. Lemere and Y. C. Tang, *Nucl. Phys.* **286**, 53(1977).
  - [8] A. B. Volkov, *Nucl. Phys* **74**, 33 (1965).
  - [9] J. Decharge and D. Gogny, *Phys. Rev.* **C21** 1568, (1980).
  - [10] M. Beiner, H. Flocard, Nguyen van giai and P. Quentin, *Nucl. Phys.* **A 238** (1975), 29.
  - [11] E. Chabanat, P. Bonche, P. Haensel, J. Meyer, R. Schaeffer, *Nucl. Phys.* **A635**, 231 (1998).
  - [12] T. Ando, K. Ikeda and A. Tohsaki, *Prog. Theory. Phys.* **64**, 1608 (1980).
  - [13] A. Tohsaki, *Phys. Rev.* **C49**, 1814 (1994).
  - [14] M. Kamimura, *Prog. Theor. Phys. Suppl.* No. 62, 236 (1978).
  - [15] S. Okabe and Y. Abe, *Prog. Theor. Phys.* **61**, 1049 (1979).
  - [16] R. Nilson, W. K. Jentschke, G. R. Briggs, R. O. Kerman and J. N. Snyder, *Phys. Rev.* **109**, 850 (1958); T. A. Tombrello and L. S. Senhouse, *Phys. Rev.* **129**, 2252 (1963); N. P. Heydenberg and G. M. Temmer, *Phys. Rev.* **104**, 123 (1956); W. S. Chien and R. E. Brown, *Phys. Rev.* **C10**, 1767 (1974).
  - [17] Y. Kanada-En'yo, *Phys. Rev. Lett.* **81**, 5291 (1998).
  - [18] N. Yamaguchi, T. Kasahara, S. Nagata and Y. Akaishi, *Porg. Theor. Phys.* **62**, 1018 (1979).

- [19] Y. Sugawa, M. Kimura and H.Horiuchi, Prog. Theor. Phys. **106**, 1129 (2001).
- [20] G. Fricke, C. Bernhardt, K. Heilig, L. A. Schaller, L. Schellenberg, E. B. Shera and C. W. Dejager, Atomic Data and Nucl. Data Tabl. **60**, 177 (1995).
- [21] A.Ozawa, T.Suzuki, I.Tanihata, Nucl. Phys. **A693**, 32 (2001).
- [22] J. P. Blaizot, Phys. Rep. **64**. 171(1980); J. P. Blaizot et al., Nucl.Phys. **A591**, 435 (1995).
- [23] G. Colò, P. F. Bortignon, N. Van Gai, A. Bracco, and R. A. Broglia, Phys. Lett. B **276**, 279(1992).
- [24] D. H. Youngblood, H. L. Clark, and Y. -W. Lui, Phys. Rev. Lett. **82**, 691 (1999).
- [25] G. A. Lalazissis, J. König, and P. Ring, Phys. Rev. **C55**, 540 (1997).
- [26] H. A. Bethe, Ann. Rev. Nucl. Sci. **23**, 93 (1971).